Comparative Mössbauer and magnetization study of 1% ^{119}Sn-doped $La_{0.67}Ca_{0.33}MnO_3$ and $La_{0.67}Sr_{0.33}MnO_3$

E. Assaridis,[1] I. Panagiotopoulos,[2] A. Moukarika,[1] and T. Bakas[1,*]
[1]*Physics Department, University of Ioannina, P.O. Box 1186, GR-451 10, Ioannina, Greece*
[2]*Department of Materials Science and Engineering, University of Ioannina, P.O. Box 1186, GR-451 10, Ioannina, Greece*
(Received 23 December 2006; revised manuscript received 31 March 2007; published 13 June 2007)

A detailed comparative Mössbauer study of $La_{0.67}Ca_{0.33}MnO_3$ and $La_{0.67}Sr_{0.33}MnO_3$ samples doped with 1% Sn is presented. The spectra at 5 K can be analyzed by a single ferromagnetic component. However, at higher temperatures two separate ferromagnetic components and a paramagnetic one are required to fit the spectra. The ferromagnetic component with the lower hyperfine field is attributed to clusters of weakened double-exchange interactions due to competition by localization mechanisms. Clear differences between the two samples in regard to the critical behavior arise: (i) The hyperfine field of $La_{0.67}Ca_{0.33}Mn_{0.99}Sn_{0.01}O_3$ disappears abruptly at T_c in contrast to that of $La_{0.67}Sr_{0.33}Mn_{0.99}Sn_{0.01}O_3$ which varies continuously and goes to zero smoothly at the critical temperature. (ii) The second ferromagnetic phase appears above $0.35T_c$ in the Ca sample but only above $0.83T_c$ in the Sr sample. The paramagnetic component appears for $T>0.67T_c$ in the former compared to $T>0.9T_c$ in the latter. The results support recent studies that show differences in the polaronic character, and critical behavior thereof, between the two materials.

DOI: 10.1103/PhysRevB.75.224412 PACS number(s): 75.47.Lx, 76.80.+y, 75.47.Gk

I. INTRODUCTION

The report of so-called colossal magnetoresistance (CMR) effects in mixed-valence perovskite manganites, associated with a simultaneous ferromagnetic to paramagnetic and metal insulator transition near optimal doping, has instigated an intensive research effort on these materials.[1] However, in these materials the strong coupling between the charge, spin, and lattice degrees of freedom gives rise to a rich phase diagram in a wide temperature and composition range which is of great interest from the condensed matter physics point of view. Thus, a relatively small fraction of the existing vast amount of literature has been focused on the nature of the transition itself and often with controversial views.[2–14] Efforts to get a deeper knowledge of the thermodynamics of the transition have been based on the study of macroscopic quantities (magnetization, heat capacity, specific heat, thermal expansion),[2–9] as well as on the techniques that can probe spin dynamics and the order parameter in a microscopic level.[10–14]

It is reasonable to expect that the connection between transport and magnetic order, due to the double-exchange mechanism and the electron-phonon coupling through the Jahn-Teller effect, should lead to a transition different from that of conventional ferromagnets, giving rise to the appearance of CMR. It has been reported that the order of the ferromagnetic transition may differ between different compositions,[4,5,8,11,13,15] having different critical temperatures, and that this may also be correlated to the magnitude of CMR near the T_c, which, as a rule of thumb, is inversely related to the T_c value.[16] Thus the nonconventional character of the magnetic transition might be related to the exact nature of double-exchange interactions, the electron-phonon coupling, and the formation of magnetic polarons which can be observed at temperatures away from T_c.

According to numerous reports, the ferromagnetic (FM) metallic phase separates into FM insulating (FI) and FM metallic phases either intrinsically or due to sensitivity to chemical disorder near first-order transitions.[17–24] Using Mössbauer spectroscopy, it was found[25,26] that the FM metallic phase in ^{57}Co-substituted $La_{1-x}Ca_xMnO_3$ ($x\sim0.3$) has a complex character; at least two spatially separated FM regions exist, which possess temperature-dependent volumes and different internal hyperfine fields. An unconventional critical behavior, with a discontinuous loss of long-range ferromagnetic ordering via the formation of small magnetic clusters exhibiting superparamagneticlike behavior around the critical temperature T_c, is reported.[25,26] When an external magnetic field is applied, the clusters coalesce into larger ones having a higher degree of spin order. This process provides an appealing explanation of the CMR effect and the dependence of its magnitude on the nature of the transition.

In this paper, we report a detailed comparative Mössbauer study of $La_{0.67}Ca_{0.33}MnO_3$ and $La_{0.67}Sr_{0.33}MnO_3$ samples doped with 1% ^{119}Sn. The samples were chosen to represent two exemplary compositions near optimal doping (33% in alkali metal) but with different critical temperatures (T_c =230 and T_c=355 K, respectively) and CMR magnitudes. Earlier reports, based on macroscopic measurements, indicated that $La_{0.67}Ca_{0.33}MnO_3$ shows a first-order transition whereas higher-T_c materials such as $La_{0.67}Sr_{0.33}MnO_3$ and $La_{0.67}Ba_{0.33}MnO_3$ follow a more conventional ferromagnetic transition.[4,5] The differences between the above two compositions are supported by more recent reports which show the presence of a distinct kind of polarons[27] and the existence of a mechanism of phase separation into hole-rich itinerant-electron and hole-poor polaronic regions in Ca-containing samples, which suppresses the ferromagnetic double exchange.[28] The Sn ions substitute Mn^{4+} and serve as a probe of the magnetic state of the host lattice via the transferred hyperfine interactions from its neighboring Mn magnetic ions. The aim is to observe microscopically the temperature evolution of the different magnetic components and especially in the vicinity of the critical temperature.

II. EXPERIMENT

$La_{0.67}Ca_{0.33}Mn_{0.99}Sn_{0.01}O_3$ and $La_{0.67}Sr_{0.33}Mn_{0.99}Sn_{0.01}O_3$ samples were prepared by a standard solid-state reaction from stoichiometric amounts of high-purity La_2O_3 (99.999%, Aldrich), $SrCO_3$ (99.995%, Aldrich), $BaCO_3$ (99.995%, Aldrich), $CaCO_3$ (99.995%, Aldrich), Mn_2O_3 (99.999%, Aldrich), and SnO_2 (enriched in ^{119}Sn) powders, sintered at 1380 °C for 8 days with three intermediate grindings. X-ray powder diffraction (XRD) diagrams were collected with a Bruker D8 Advance Diffractometer using Cu $K\alpha$ ($\lambda = 1.5418$ Å) and a secondary graphite monochromator, in 2θ mode from 10° to 120° with steps of 0.02° and 10-s/step accumulation time. Magnetic measurements were performed on a Lakeshore 3700 vibrating-sample magnetometer (VSM). The electrical resistance measurements were performed with a four-probe method and with the current parallel to the applied magnetic field in the cryostat of a superconducting quantum interference device (SQUID) magnetometer (Quantum Design) with the EDC option. Mössbauer spectra were recorded with a conventional constant-acceleration spectrometer. The source (5 mCi, $CaSnO_3$) was at room temperature (RT), while the absorbers were kept fixed at the desired temperature (4.2–360 K) with the aid of an exchange gas cryostat or a Mössbauer furnace. The spectra were analyzed with a least-squares computer minimization procedure, assuming Lorentzian line shapes.

III. RESULTS

The refinement of the XRD patterns was carried out by the Fullprof Rietveld program.[29] The two samples were verified to be single phase, with a structure that can be described by a rhombohedral unit cell (space group $R\text{-}3C$) for $La_{0.67}Sr_{0.33}Mn_{0.99}Sn_{0.01}O_3$ and an orthorhombic unit cell (space group *Pnma*) for $La_{0.67}Ca_{0.33}Mn_{0.99}Sn_{0.01}O_3$ (Fig. 1). The refined structural parameters for the two samples are listed in Table I.

Macroscopic magnetization measurements indicate that the critical behavior of the two samples is different, in accordance with previous studies.[4,5,13] Arrott plots for the two samples are presented in Fig. 2. According to the Landau theory of second-order transitions, the magnetization M for isotherms close to the critical point has a linear dependence on H/M, where H is the external magnetic field. In the case of the Sr-containing sample, a typical second-order behavior is observed. The critical exponents $\beta=0.453$ and $\gamma=1.10$ have been determined by the construction of generalized Arrott plots. In contrast, for the Ca-containing sample, strong deviations from linearity are observed, which cannot be compromised by any choice of β and γ. Furthermore, several isotherms around the Curie point show negative slopes in some parts, which, according to the Banerjee's criterion, is an indication of the first-order character of the transition.[5,30] However, in these materials, in which there is a strong coupling of magnetism with other degrees of freedom, such as lattice and charge, the validity of this approach[15] and even the role of magnetization as the order parameter[9] have been questioned. Thus, we have used Mössbauer spectroscopy as a tool to monitor locally the magnetic order and spin dynamics at low temperatures as well as close to the critical temperature.

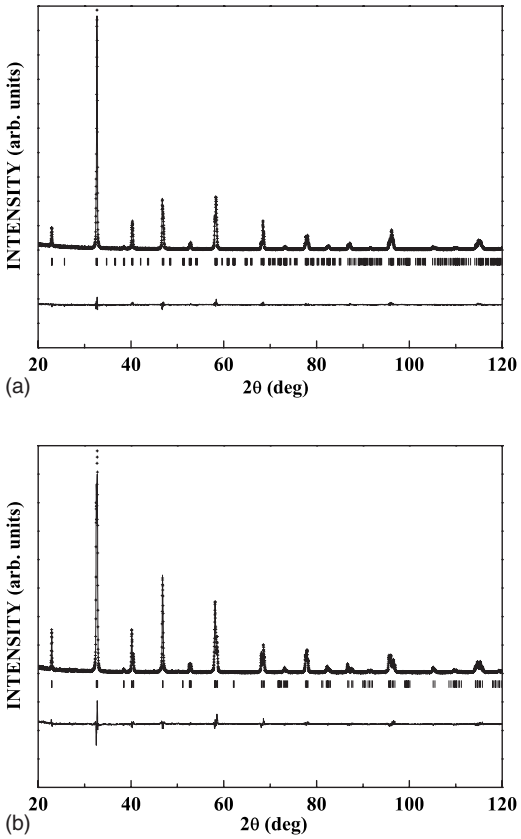

FIG. 1. Rietveld refinement of the XRD patterns for the samples (a) $La_{0.67}Ca_{0.33}Mn_{0.99}Sn_{0.01}O_3$ and (b) $La_{0.67}Sr_{0.33}Mn_{0.99}Sn_{0.01}O_3$.

Magnetically split Mössbauer spectra are observed well below the critical temperature, which is 230 K for $La_{0.67}Ca_{0.33}Mn_{0.99}Sn_{0.01}O_3$ and 355 K for $La_{0.67}Sr_{0.33}Mn_{0.99}Sn_{0.01}O_3$. Approaching the critical temperature, from below, a paramagnetic component evolves, the area of which increases at the cost of the magnetic ones. Representative spectra are shown in Figs. 3(a) and 3(b).

The ^{119}Sn Mössbauer spectra for the $La_{0.67}Ca_{0.33}Mn_{0.99}Sn_{0.01}O_3$ and $La_{0.67}Sr_{0.33}Mn_{0.99}Sn_{0.01}O_3$ samples, at 230 and 355 K, consist of a single absorption line with full width at half maximum (FWHM) $=0.78(1)$ mm/s and isomer shift 0.12(1) mm/s. The latter value corresponds to a 4+ valence state of Sn, indicating that Sn ions substitute Mn^{4+} ions.[18]

The hyperfine magnetic fields measured below the critical temperature are those sensed by the Sn nucleus from the overlapping of the $3d$ orbitals of its Mn neighbors in the surrounding Mn octahedron with its $5s$ orbitals. The isomer shift value for Ca and Sr samples is 0.15 mm/s for both magnetic components and ΔEq is practically 0.00 mm/s. No changes were observed in the isomer shift values, apart from those arising from the second-order Doppler shift, as well as in the quadrupole splitting values, in the whole temperature range for the two samples.

The crystal symmetry allows a single-crystallographic Mn site for both $La_{0.67}Ca_{0.33}Mn_{0.99}Sn_{0.01}O_3$ and

TABLE I. Lattice constants of the $La_{0.67}Ca_{0.33}Mn_{0.99}Sn_{0.01}O_3$ and $La_{0.67}Ca_{0.33}Mn_{0.99}Sn_{0.01}O_3$ samples. Numbers in parentheses are errors of the last significant digit.

	a (Å)	b (Å)	c (Å)	Volume (Å^3)	Space group
$La_{0.67}Sr_{0.33}Mn_{0.99}Sn_{0.01}O_3$	5.5041(1)	5.5041(1)	13.362(3)	350.574(1)	*R*-3*C*
$La_{0.67}Ca_{0.33}Mn_{0.99}Sn_{0.01}O_3$	5.4614(1)	7.7168(3)	5.4743(1)	230.714(1)	*Pnma*

$La_{0.67}Ca_{0.33}Mn_{0.99}Sn_{0.01}O_3$ structures. Accordingly, analysis of the 4.2 K spectra can be successfully performed by considering just one magnetically split component in each case. At 78 K the Mössbauer spectrum of the Sr sample can be fitted with one magnetic component while the Ca sample requires two separate magnetic components. The relatively large values of the hyperfine fields of these components ($H_{hf} \approx 27.7$ T for the main magnetic component in the case of $La_{0.67}Ca_{0.33}Mn_{0.99}Sn_{0.01}O_3$ and $H_{hf} \approx 33.2$ T in the case of $La_{0.67}Sr_{0.33}Mn_{0.99}Sn_{0.01}O_3$) show that they originate from an environment where all the Mn moments are parallel (FM component). In the Ca-sample spectra, the reduced hyperfine field values of the second component, with respect to the main ferromagnetic one, allows us to suppose that this magnetic component also comes from a ferromagnetic environment with reduced interactions, which might be related to less mobile charges.[31]

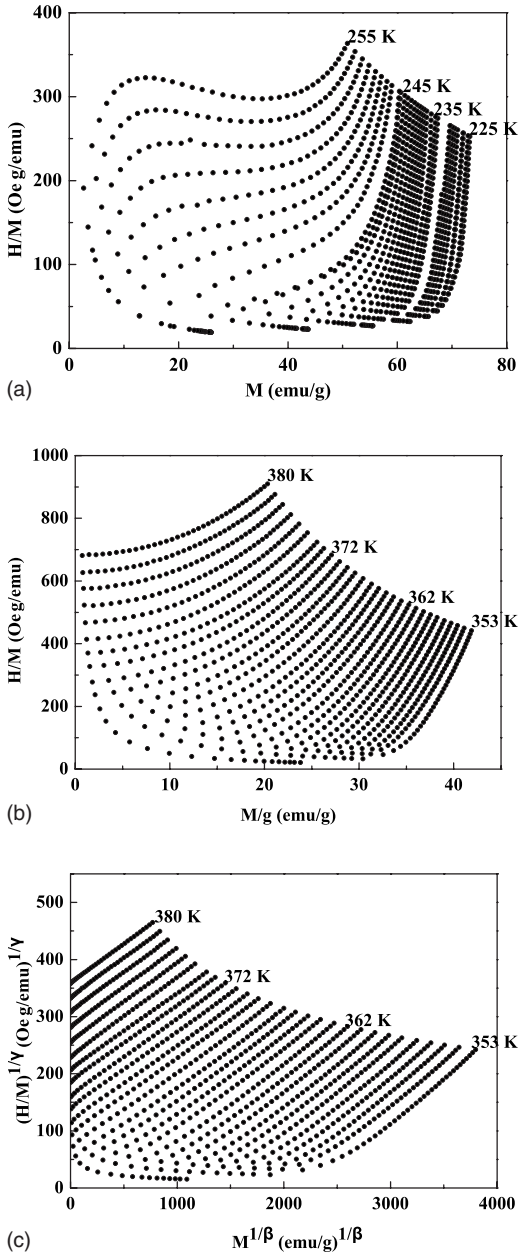

FIG. 2. Arrott plots for the samples (a) $La_{0.67}Ca_{0.33}Mn_{0.99}Sn_{0.01}O_3$, (b) $La_{0.67}Sr_{0.33}Mn_{0.99}Sn_{0.01}O_3$, and (c) modified Arrott plots for the sample $La_{0.67}Sr_{0.33}Mn_{0.99}Sn_{0.01}O_3$.

Based on (a) the tendency of this component to increase, at the expense of the higher-field one around the critical temperature, and (b) its stronger presence in the Ca-containing sample (for which macroscopic measurements show a less conventional critical behavior), we attribute this component to the effects of polaronic localization of the charge carriers: Recent studies by Raman spectroscopy[28] support phase separation into hole-rich, itinerant-electron, and hole-poor polaronic regions, although a localization mechanism that sets in when the characteristic time for an electron to hop from a Mn^{3+} to a Mn^{4+} ion becomes comparable to $1/\omega_0$ where ω_0 is the period of the optical-mode vibration of the MnO_3 array. This explains the low T_c values compared to the adiabatic ones, which can be estimated by the double-exchange model according to the bandwidth dependence on the Mn-O-Mn bond angle. It is thus reasonable to assume that the second ferromagnetic component appears as a result of the competition between double-exchange and localization mechanisms which leads to regions of reduced ferromagnetic exchange. These are maximized at the transition region since they finally evolve into fully localized paramagnetic regions at higher temperatures.

For the Ca-containing sample, the lattice is characterized by a smaller tolerance factor and it is therefore more prone to the formation of polarons, compared to the Sr sample lattice, which has a tolerance factor close to unity. The contrast in the critical behavior between the two samples can also be seen by the fact that long-range magnetic order breaks down with the appearance of the paramagnetic component above $T/T_c \sim 0.67$ in the case of the $La_{0.67}Ca_{0.33}Mn_{0.99}Sn_{0.01}O_3$ sample and above $T/T_c \sim 0.90$ in the case of the $La_{0.67}Sr_{0.33}Mn_{0.99}Sn_{0.01}O_3$. The temperature variation of the relative intensity of each component is presented in Fig. 4. In the Sr sample the second ferromagnetic component appears above 295 K ($0.83T_c$) compared to 78 K ($0.35T_c$) for the Ca sample.

In Fig. 5 the temperature dependence of the hyperfine fields of the two ferromagnetic components that appear in the Mössbauer spectra is sketched, revealing a striking contrast

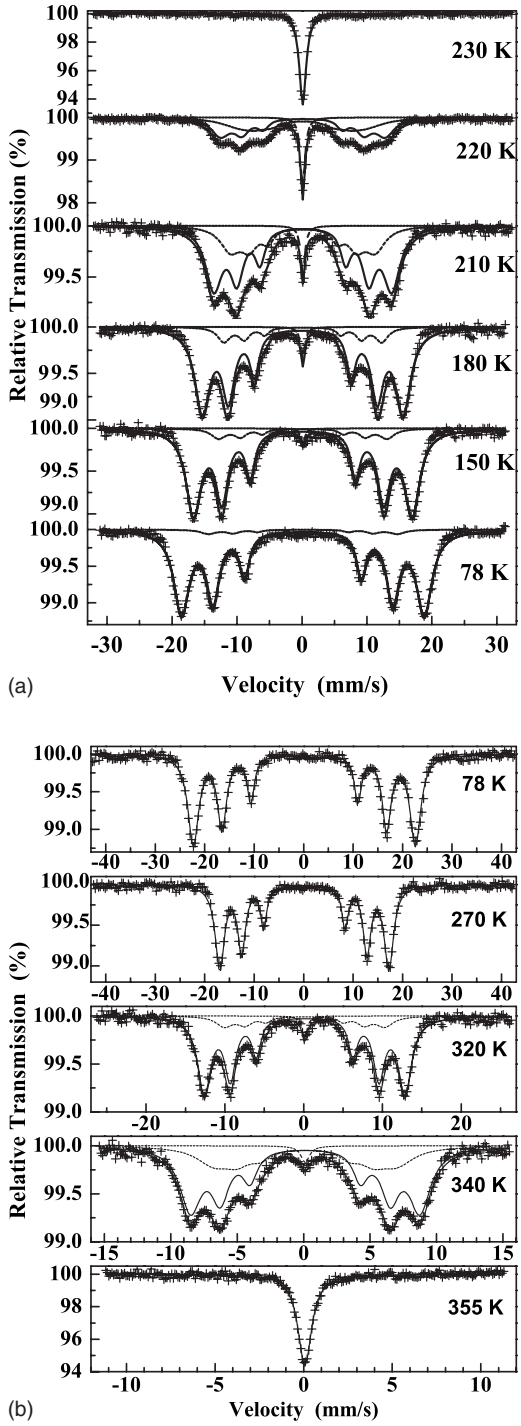

FIG. 3. Mössbauer spectra for the samples (a) $La_{0.67}Ca_{0.33}Mn_{0.99}Sn_{0.01}O_3$ and (b) $La_{0.67}Sr_{0.33}Mn_{0.99}Sn_{0.01}O_3$ at the different temperatures indicated.

between the two samples: while in the case of $La_{0.67}Sr_{0.33}Mn_{0.99}Sn_{0.01}O_3$ both components decrease continuously towards zero near the critical temperature, they seem to disappear abruptly in the $La_{0.67}Ca_{0.33}Mn_{0.99}Sn_{0.01}O_3$ sample. These results are in accordance with recent neutron scattering experiments performed on $La_{0.7}Ca_{0.3}MnO_3$ single crystals that show that the ferromagnetic phase is truncated by the formation of polarons,[14] which cause an abrupt transition to the paramagnetic insulating state, while in the case of $La_{0.8}Ca_{0.2}MnO_3$ single crystal, a typical second-order transition behavior is observed.

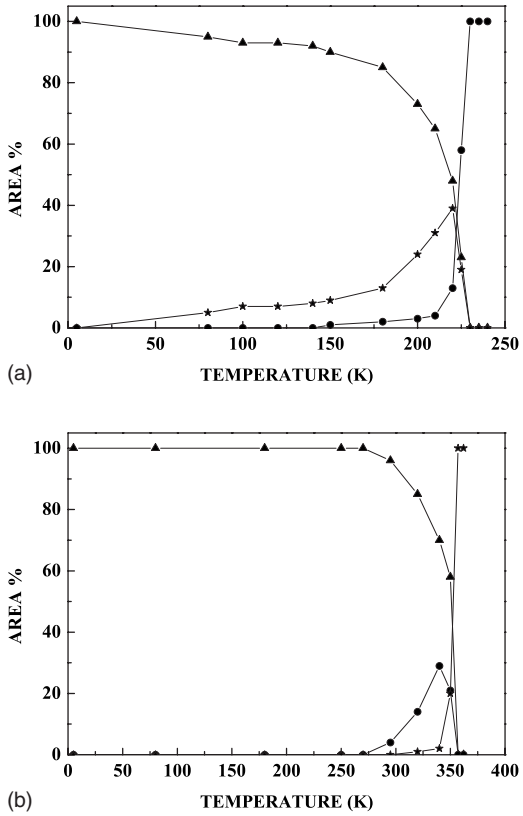

FIG. 4. Temperature variation of the relative areas of the components, after analysis of the Mössbauer spectra for the samples (a) $La_{0.67}Ca_{0.33}Mn_{0.99}Sn_{0.01}O_3$ and (b) $La_{0.67}Sr_{0.33}Mn_{0.99}Sn_{0.01}O_3$ (▲, main magnetic component; ●, magnetic component; ★, paramagnetic component).

Lately several works have focused on the description of the metal-insulator transition in manganites as a percolative transition.[33] The electrical resistance of $La_{0.67}Ca_{0.33}Mn_{0.99}Sn_{0.01}O_3$ as a function of temperature under zero field compared to that in an applied field of 5 T is shown in Fig. 6. The difference between the two curves corresponds to a maximum magnetoresistance of 325% at 230 K. Since the analysis of our spectra involves the simultaneous presence of different phases, it suggests a percolative nature of the transition.[24] It is thus tempting to compare the temperature dependence of the resistivity, $\rho(T)$, against the fractions of the different components (ferromagnetic, cluster, paramagnetic) at each temperature which we denote as $f(T)$, $c(T)$, and $p(T)$, respectively. At temperatures below $T_c/2 \approx 110$ K we find the data can be fitted to the empirical law $\rho_{met}(T)=\rho(0)+\rho_1 T^{2.5}$.[32]

However, as can been seen in Fig. 6, this relation describes the data up to 200 K. This is not surprising since within this temperature interval the ferromagnetic component dominates $f>0.73$. The temperature where the resistivity peak is observed agrees with the temperature above which the sample is fully paramagnetic according to the analysis of the spectra. Above 230 K the temperature depen-

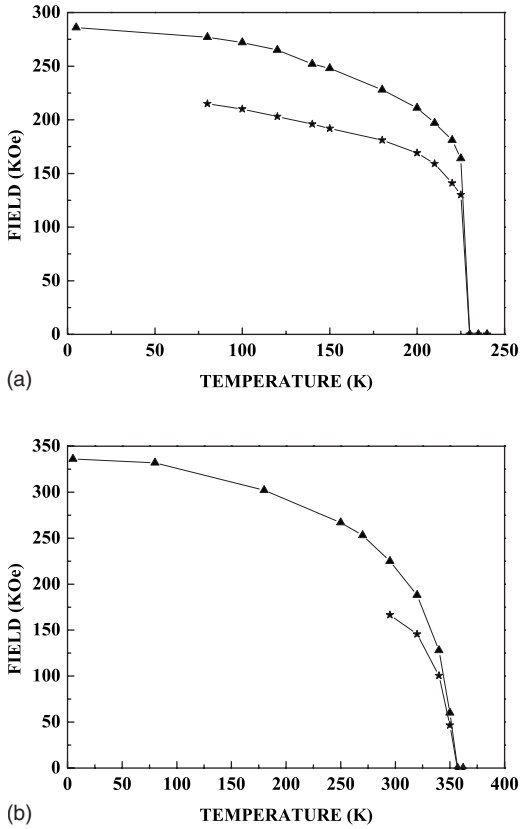

FIG. 5. Temperature variation of hyperfine fields of the magnetic components of the Mössbauer spectra for the samples (a) $La_{0.67}Ca_{0.33}Mn_{0.99}Sn_{0.01}O_3$ and (b) $La_{0.67}Sr_{0.33}Mn_{0.99}Sn_{0.01}O_3$ (▲, main magnetic component; ●, second magnetic component).

dence can be fitted to an activated behavior $\rho_{para}(T) = C\exp(E_g/kT)$ with $E_g/k = 230$ K. That leaves only a narrow temperature interval 200 K $< T <$ 230 K in which all three components coexist in appreciable amounts and $\rho(T)$ ceases to be trivial. An attempt to extent the temperature dependences $\rho_{met}(T)$ and $\rho_{para}(T)$, found for the metallic and the paramagnetic phases in the temperature region within each one dominates, in the interval where all the components coexist can be made using a simple mixing rule of the form $\rho = \rho_{met}(T)[1-p(T)] + \rho_{para}(T)p(T)$. The thus calculated values are plotted in Fig. 6 (as solid squares) and show a fair agreement with the data in the interval 200 K $< T <$ 230 K but an apparent deviation in the interval 150 K $< T <$ 200 K. This deviation signifies that this simple mixing rule overestimates the effect of the existence of the paramagnetic phase in small fractions which cannot have any effect on the percolation through the metallic component. Better agreement in this region can be found by the following approximation: For a fraction x of a highly resistive component dispersed in a conducting matrix the effective resistivity of the composite can be written as $\rho = \rho_{matrix}(1+x/2)/(1-x)$.[34] Applying this approach we find that the quantity $\rho = \rho_{met}(T) \times [1+p(T)/2]/[1-p(T)]$ gives a better description of the data for low fractions of the paramagnetic component. The calculated values are also plotted in Fig. 6 (as solid triangles). The previous relations imply that the second ferromagnetic component should be assigned a resistivity value closer to that of the main ferromagnetic one than to the paramagnetic. If, for instance, a mixing rule of the form $\rho = \rho_{met}(T)f(T) + \rho_{para}(T)[1-f(T)]$ is used, there is no agreement with the experimental data.

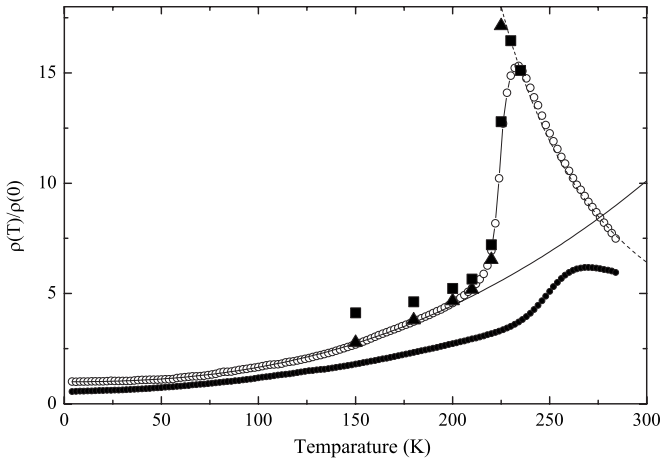

FIG. 6. Electrical resistivity of $La_{0.67}Ca_{0.33}Mn_{0.99}Sn_{0.01}O_3$ as a function of temperature under zero field (open circles) and under an applied field of 5 T (solid circles). The dashed line represents a fit according to the empirical relation $\rho_{met}(T) = \rho(0) + \rho_1 T^{2.5}$. Solid triangles represent the quantity $\rho_{met}(T)[1+0.5\cdot p(T)]/[1-p(T)]$ where $p(T)$ is the temperature-dependent fraction of the paramagnetic phase as estimated by Mössbauer spectroscopy. Solid squares represent the quantity $\rho_{met}(T)[1-p(T)] + \rho_{para}(T)p(T)$ where $\rho_{para}(T) = C\exp(E_g/kT)$ (represented by the dashed line).

Despite the above-mentioned differences between the Ca and Sr samples the scenario of a clear distinction between a first-order transition for the former and a second-order one for the latter cannot be strongly supported by the above data since in both samples (a) a second magnetic component, which increases near T_c, is observed and (b) the paramagnetic component becomes apparent well below T_c in both samples. As already mentioned, the six-coordinated Mn^{4+} is replaced by Sn^{4+}, but it known that Sn^{4+} has a higher ionic radius than Mn^{4+} (Mn^{4+}, 0.53 Å; Sn^{4+}, 0.69 Å). It is therefore expected to locally distort the structure. Moreover, Sn^{4+} ions disrupt the double-exchange transfer mechanism and act as nonmagnetic impurities. It is therefore very likely that magnetic polarons occur preferentially around the Sn atoms, leading to an enhancement of the apparent "polaronic" component in the spectra with respect to the actually occurring one.

In summary a detailed comparative Mössbauer study of $La_{0.67}Ca_{0.33}MnO_3$ and $La_{0.67}Sr_{0.33}MnO_3$ samples doped with 1% ^{119}Sn has been presented. The Ca sample, compared to the Sr one, has a lower T_c, a lower tolerance factor, and an unconventional ferromagnetic transition according to macroscopic magnetic measurements (Arrott plots). Mössbauer studies show that in both samples as the temperature ascends approaching T_c, a second magnetic component with lower hyperfine field is observed. This is attributed to weaker exchange interactions between Mn^{3+} and Mn^{4+} due to the slower rate of double-exchange electron transfer. However, clear differences between the two samples, as regards

the critical behavior, have been observed: (i) The two samples have different critical temperatures: 230 K for $La_{0.67}Ca_{0.33}Mn_{0.99}Sn_{0.01}O_3$ and 355 K for $La_{0.67}Sr_{0.33}Mn_{0.99}Sn_{0.01}O_3$. (ii) In the Ca sample the polaronic phase is observed even at low temperatures (down to $0.35T_c$) but the in Sr sample only close to the critical temperature ($0.83T_c$). (iii) For the Ca sample the paramagnetic component appears well below T_c ($T/T_c \sim 0.67$) and for the Sr sample at $T/T_c \sim 0.90$. (iv) The hyperfine field of $La_{0.67}Ca_{0.33}Mn_{0.99}Sn_{0.01}O_3$ disappears abruptly at T_c in contrast to that of $La_{0.67}Sr_{0.33}Mn_{0.99}Sn_{0.01}O_3$ which varies continuously and goes to zero smoothly at the critical temperature.

ACKNOWLEDGMENTS

This research was funded by the program "Heraklitos" of the Operational Program for Education and Initial Vocational Training of the Hellenic Ministry of Education under the 3rd Community Support Framework and the European Social Fund. The authors would like to acknowledge the use of XRD and VSM units of the Laboratory Network, UOI.

*Author to whom correspondence should be addressed. Physics Department, University of Ioannina, P.O. Box 1186, GR-451 10, Ioannina, Greece FAX: (+)30 26510 98690. tbakas@cc.uoi.gr

[1] See, for instance, J. M. D. Coey, M. Viret, and S. Von Molnár, Adv. Phys. **48**, 167 (1999); M. B. Salamon and M. Jaime, Rev. Mod. Phys. **73**, 583 (2001).
[2] Guo-Meng Zhao, M. B. Hunt, and H. Keller, Phys. Rev. Lett. **78**, 955 (1997).
[3] K. Ghosh, C. J. Lobb, R. L. Greene, S. G. Karabashev, D. A. Shulyatev, A. A. Arsenov, and Y. Mukovskii, Phys. Rev. Lett. **81**, 4740 (1998).
[4] N. Moutis, I. Panagiotopoulos, M. Pissas, and D. Niarchos, Phys. Rev. B **59**, 1129 (1999).
[5] J. Mira, J. Rivas, F. Rivadulla, C. Vázquez-Vázquez, and M. A. López-Quintela, Phys. Rev. B **60**, 2998 (1999).
[6] J. E. Gordon, C. Marcenat, J. P. Franck, I. Isaac, Guanwen Zhang, R. Lortz, C. Meingast, F. Bouquet, R. A. Fisher, and N. E. Phillips, Phys. Rev. B **65**, 024441 (2001).
[7] D. Kim, B. L. Zink, F. Hellman, and J. M. D. Coey, Phys. Rev. B **65**, 214424 (2002).
[8] D. Kim, B. Revaz, B. L. Zink, F. Hellman, J. J. Rhyne, and J. F. Mitchell, Phys. Rev. Lett. **89**, 227202 (2002).
[9] J. A. Souza, Yi-Kuo Yu, J. J. Neumeier, H. Terashita, and R. F. Jardim, Phys. Rev. Lett. **94**, 207209 (2005).
[10] R. H. Heffner, L. P. Le, M. F. Hundley, J. J. Neumeier, G. M. Luke, K. Kojima, B. Nachumi, Y. J. Uemura, D. E. MacLaughlin, and S-W. Cheong, Phys. Rev. Lett. **77**, 1869 (1996).
[11] J. A. Fernandez-Baca, P. Dai, H. Y. Hwang, C. Kloc, and S-W. Cheong, Phys. Rev. Lett. **80**, 4012 (1998).
[12] J. W. Lynn, R. W. Erwin, J. A. Borchers, Q. Huang, A. Santoro, J-L. Peng, and Z. Y. Li, Phys. Rev. Lett. **76**, 4046 (1996).
[13] P. Novák, M. Maryško, M. M. Savosta, and A. N. Ulyanov, Phys. Rev. B **60**, 6655 (1999).
[14] C. P. Adams, J. W. Lynn, V. N. Smolyaninova, A. Biswas, R. L. Greene, W. Ratcliff II, S.-W. Cheong, Y. M. Mukovskii, and D. A. Shulyatev, Phys. Rev. B **70**, 134414 (2004).
[15] S. W. Biernacki, Phys. Rev. B **68**, 174417 (2003).
[16] K. Khazeni, Y. X. Jia, Li Lu, V. H. Crespi, M. L. Cohen, and A. Zettl, Phys. Rev. Lett. **76**, 295 (1996).
[17] A. Moreo, M. Mayr, A. Feiguin, S. Yunoki, and E. Dagotto, Phys. Rev. Lett. **84**, 5568 (2000).
[18] E. Dagotto, T. Hotta, and A. Moreo, Phys. Rep. **344**, 1 (2001).
[19] T. A. Tyson, J. Mustre de Leon, S. D. Conradson, A. R. Bishop, J. J. Neumeier, H. Röder, and Jun Zang, Phys. Rev. B **53**, 13985 (1996).
[20] G. Papavassiliou, M. Fardis, M. Belesi, T. G. Maris, G. Kallias, M. Pissas, D. Niarchos, C. Dimitropoulos, and J. Dolinsek, Phys. Rev. Lett. **84**, 761 (2000).
[21] G. Papavassiliou, M. Fardis, M. Belesi, M. Pissas, I. Panagiotopoulos, G. Kallias, D. Niarchos, C. Dimitropoulos, and J. Dolinsek, Phys. Rev. B **59**, 6390 (1999).
[22] M. Uehara, S. Mori, C. H. Chen, and S.-W. Cheong, Nature (London) **399**, 560 (1999).
[23] A. Moreo, S. Yunoki, and E. Dagotto, Science **283**, 2034 (1999).
[24] M. Fäth, S. Freisem, A. A. Menovsky, Y. Tomioka, J. Aerts, and J. A. Mydosh, Science **285**, 1540 (1999).
[25] V. Chechersky, A. Nath, C. Michel, M. Hervieu, K. Ghosh, and R. L. Greene, Phys. Rev. B **62**, 5316 (2000).
[26] V. Chechersky, A. Nath, I. Isaac, J. P. Franck, K. Ghosh, Hong-lyoul Ju, and R. L. Greene, Phys. Rev. B **59**, 497 (1999).
[27] Ch. Hartinger, F. Mayr, A. Loidl, and T. Kopp, Phys. Rev. B **73**, 024408 (2006).
[28] F. Rivadulla, M. Otero-Leal, A. Espinosa, A. de Andrés, C. Ramos, J. Rivas, and J. B. Goodenough, Phys. Rev. Lett. **96**, 016402 (2006).
[29] D. B. Wiles and R. A. Young, J. Appl. Crystallogr. **14**, 149 (1981).
[30] S. K. Banerjee, Phys. Lett. **12**, 16 (1964).
[31] Joonghoe Dho, Ilryong Kim, Soonchil Lee, K. H. Kim, H. J. Lee, J. H. Jung, and T. W. Noh, Phys. Rev. B **59**, 492 (1999).
[32] P. Schiffer, A. P. Ramirez, W. Bao, and S.-W. Cheong, Phys. Rev. Lett. **75**, 3336 (1995).
[33] Ye Xiong, Shun-Qing Shen, and X. C. Xie, Phys. Rev. B **63**, 140418(R) (2001); Shuai Dong, Han Zhu, X. Wu, and J.-M. Liu, Appl. Phys. Lett. **86**, 022501 (2005); S. L. Yuan, Z. Y. Li, G. Peng, C. S. Xiong, Y. H. Xiong, and C. Q. Tang, *ibid.* **79**, 90 (2001).
[34] S. O. Kasap, *Principles of Electronic Materials and Devices* (McGraw-Hill, New York, 2001).